

Supplementary Material

Neogene mass accumulation rate of carbonate sediment across northern Zealandia, Tasman Sea, southwest Pacific

R. Sutherland¹, Z. Dos Santos¹, C. Agnini², L. Alegret³, A.R. Lam⁴, T. Westerhold⁵, M.K. Drake⁶, D.T. Harper⁷, E. Dallanave⁵, C. Newsam⁸, M.J. Cramwinkel⁹, G.R. Dickens¹⁰, J. Collot¹¹, S.J.G. Etienne¹¹, A. Bordenave¹¹, W.R. Stratford¹², X. Zhou¹³, H. Li¹⁴, G. Asatryan¹⁵

1. Victoria University of Wellington, PO Box 600, Wellington, New Zealand
2. Università di Padova, 35131 Padova, Italy
3. Universidad de Zaragoza, 50009 Zaragoza, Spain
4. University of Massachusetts Amherst, MA 01003-9297, USA
5. MARUM, University of Bremen, 28359 Bremen, Germany
6. University of California, Santa Cruz, CA 95064, USA
7. University of Kansas, Lawrence, KS 66045-7575, USA
8. University College London, London WC1E 6BT, UK
9. National Oceanography Centre, University of Southampton, Southampton SO14 3ZH, UK
10. Trinity College Dublin, Dublin 2, Ireland
11. Geological Survey of New Caledonia, Noumea BP 465, New Caledonia
12. GNS Science, PO Box 30368, Lower Hutt, New Zealand
13. Rutgers, The State University of New Jersey, NJ 08854, USA
14. Institute of Oceanology, Chinese Academy of Sciences, Qingdao, China
15. Leibniz-Institut für Evolutions und Biodiversitätsforschung, 10115 Berlin, Germany

Contact: rupert.sutherland@vuw.ac.nz

Contents

Figure S1. Borehole U208.	3
Figure S2. Borehole U1506.	4
Figure S3. Borehole U1510.	4
Figure S4. Borehole U207.	5
Figure S5. Borehole U592.	5
Figure S6. Borehole U1507.	6
Figure S7. Borehole U1508.	7

Figure S8. Southern Lord Howe Rise seismic reflection line TAN1409-LHRS-02 through borehole U1510, (A) seismic reflection image, and (B) illustrates Eocene reverse faulting, deformation, volcanism and erosional unconformity.	8
Figure S9. Southern Lord Howe Rise seismic reflection line 114_07 between Sites U592 and U207: (A) seismic reflection image, and (B) two sites show a lack of continuity of strata beneath a Miocene-Paleogene unconformity.	9
Figure S10. Southern Lord Howe Rise seismic line TAN1409-LHRS_01 near Site U592: (A) seismic reflection image, and (B) sketch of onlapping section just above Miocene unconformity (black yellow dash line).	10
Figure S11. Bathymetric map showing local setting of Site U1507, with canyons and landslide scars on the adjacent flank of Norfolk Ridge.	11
Figure S12. Seismic line line TAN1409-NCTN-11 at Site U1507, (A) seismic reflection image with horizons picked in colour, and (B) sketch of onlapping and downlapping strata near Site U1507. Stratigraphic onlaps are shown with small black arrow facing northeast and small two arrows with purple and blue colour are toplapping reflectors. Black line is polygonal faulting. Blank areas are transparent acoustically and interpreted as large-scale debris flows.	12
Figure S13. Seismic line TAN1409-011 near Site U1507 shows deposition of reworking sediment at the basin; (A) seismic reflection image, and (B) interpreted illustrating the relative position of slope failure scars at seabed and pinchout or onlap mass transport deposits at the edge of the basin, and buried escarpments on the slope.	13
Figure S14. Reinga Basin seismic reflection line REIN09-011 illustrates horizons picked and seismic units near Site U1508: (A) seismic reflection image and, (B) interpreted seismic reflection presenting key seismic stratigraphic relationship along the strike. UB-REIN-5 appeared to correspond with the base strata, UB-REIN-6 and UB-REIN-7 onlap the volcano in the SE where seabed seems scouring against the volcano.	14
Figure S15. Site U1507 calcium carbonate (black dashed, wt %) values binned by sample age, averaged, and then interpolated to fill gaps. The NCTN average MAR curve (blue; Fig. 11) is corrected using the calcium carbonate curve to determine the carbonate component of MAR (red dotted; $\text{kg kyr}^{-1} \text{m}^{-2}$).	15
Table S1. Biostratigraphy for DSDP Leg 21 revised to be consistent with Sutherland et al. (2019). B = base, T = top, Bc = base common, Tc = top common.	16
Table S2. Biostratigraphy for DSDP Leg 90 revised to be consistent with Sutherland et al. (2019). B = base, T = top.	17
Table S3. Ages assigned to reflectors, northern Lord Howe Rise.	18
Table S4. Ages assigned to reflectors, southern Lord Howe Rise.	18
Table S5. Ages assigned to reflectors, northern New Caledonia Trough.	19
Table S6. Ages assigned to reflectors, Reinga Basin.	19
References.	20

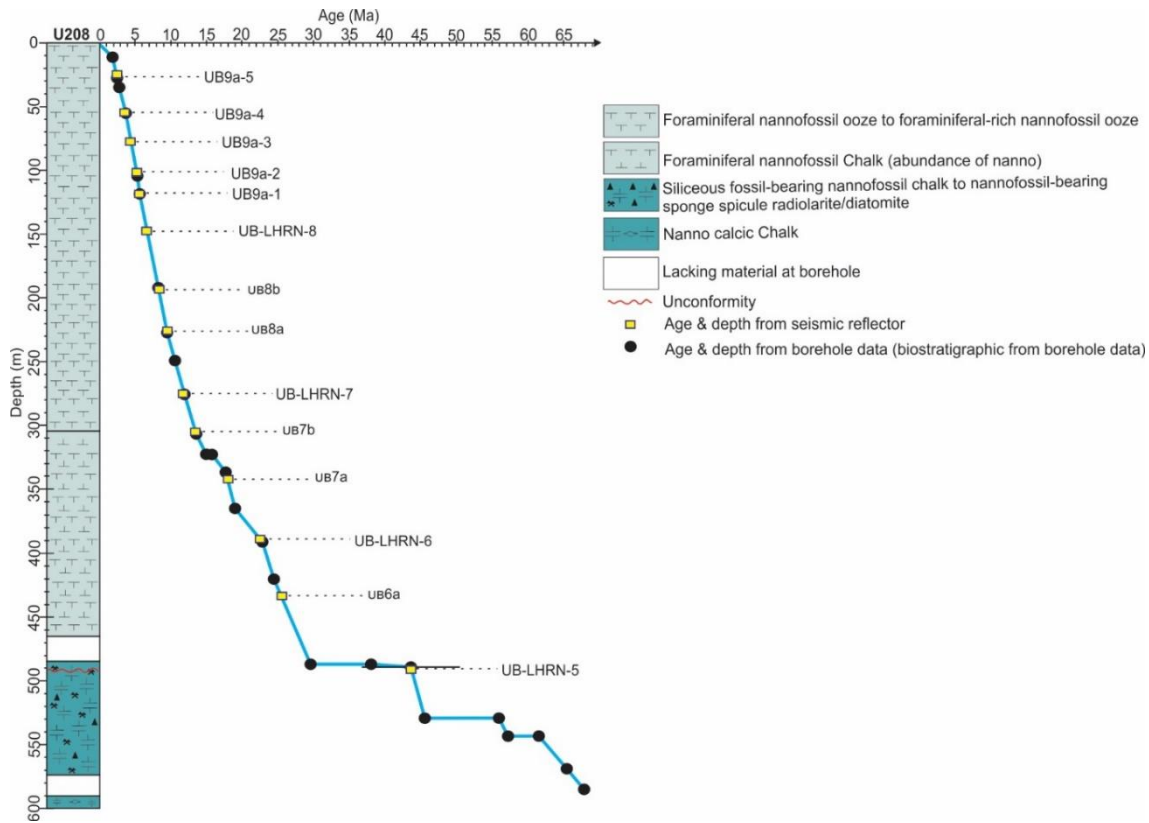


Figure S1. Borehole U208.

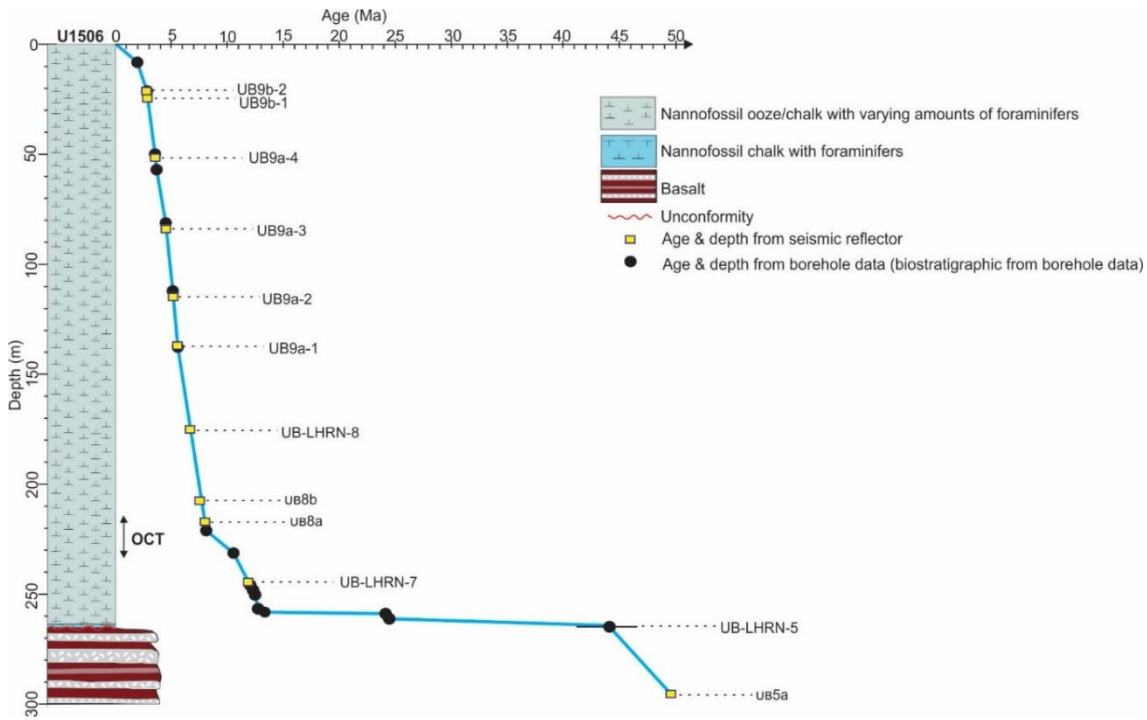


Figure S2. Borehole U1506.

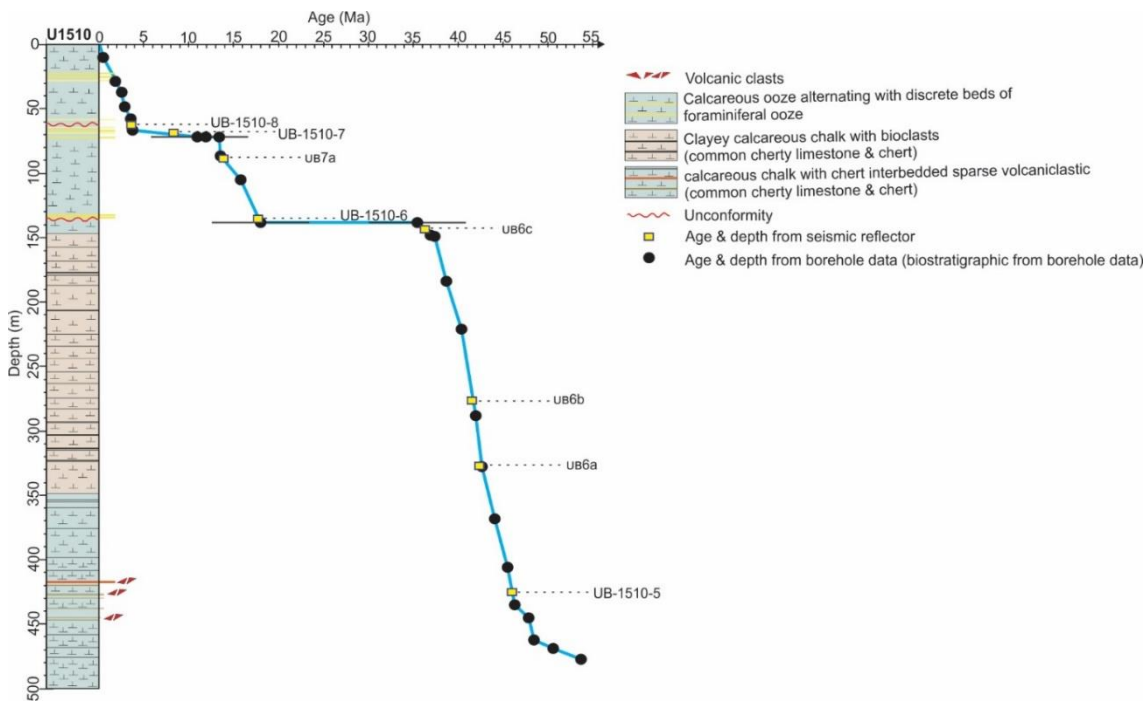


Figure S3. Borehole U1510.

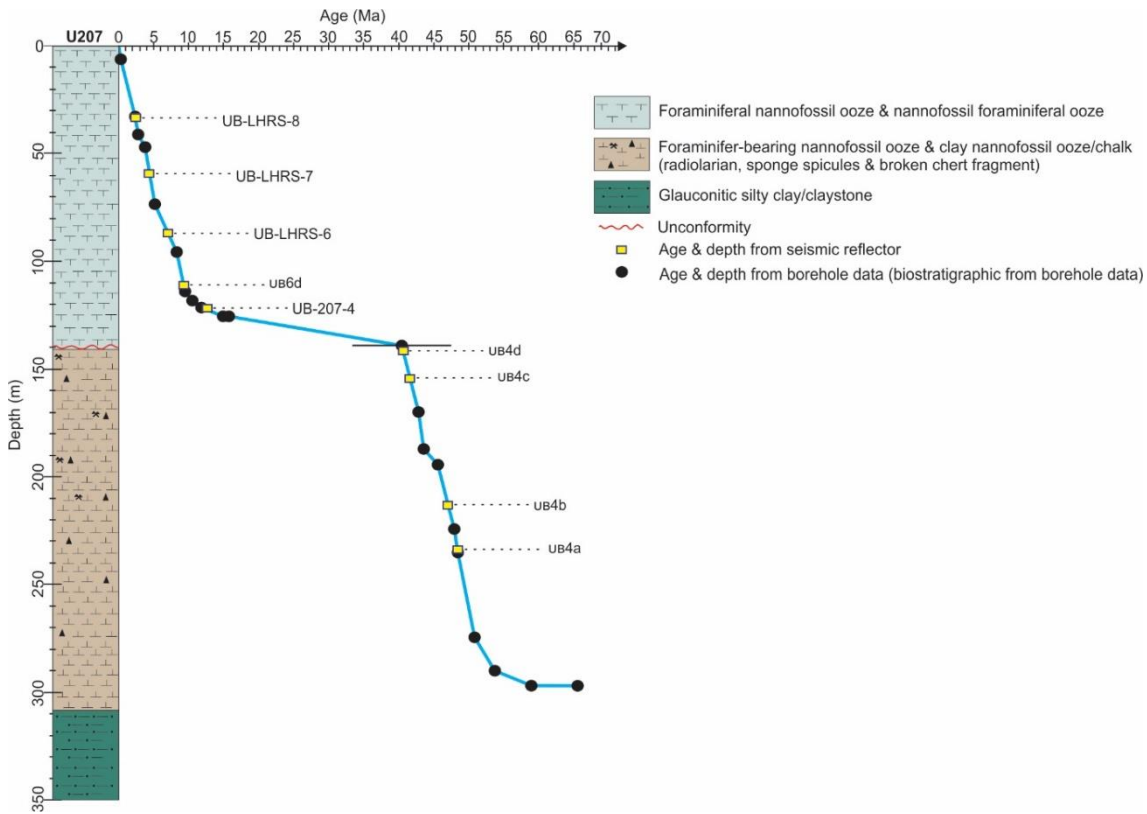


Figure S4. Borehole U207.

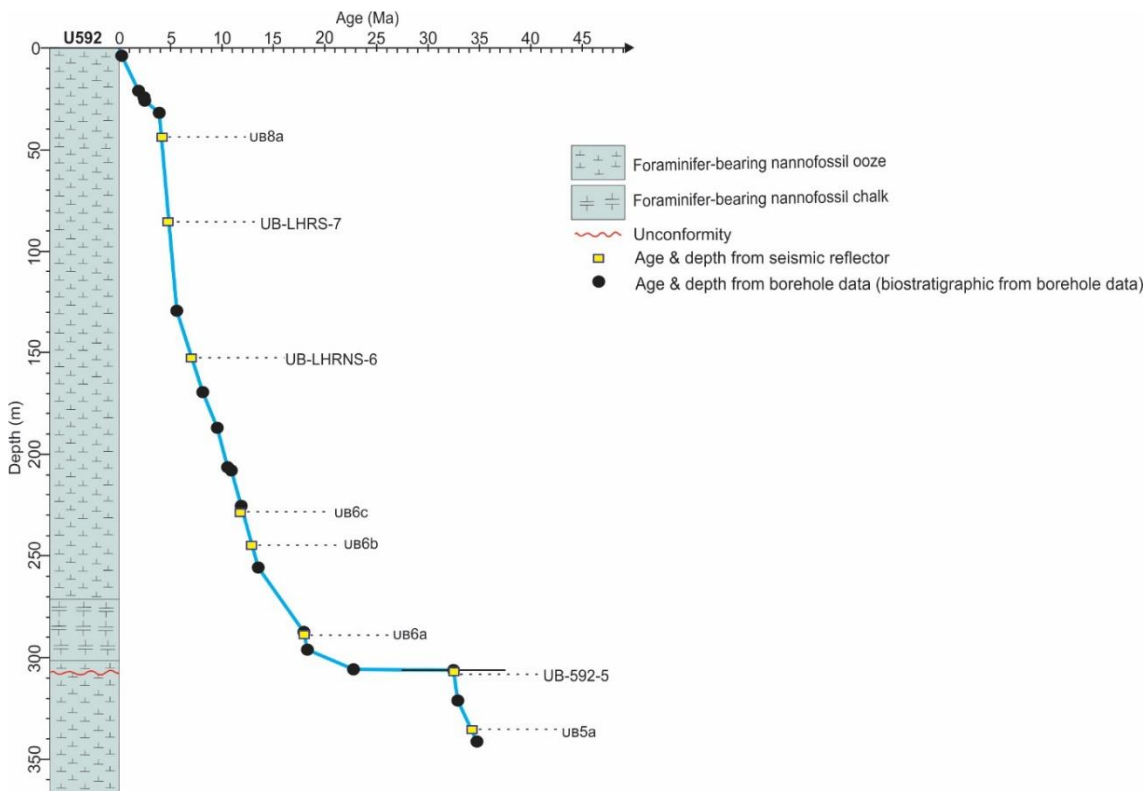


Figure S5. Borehole U592.

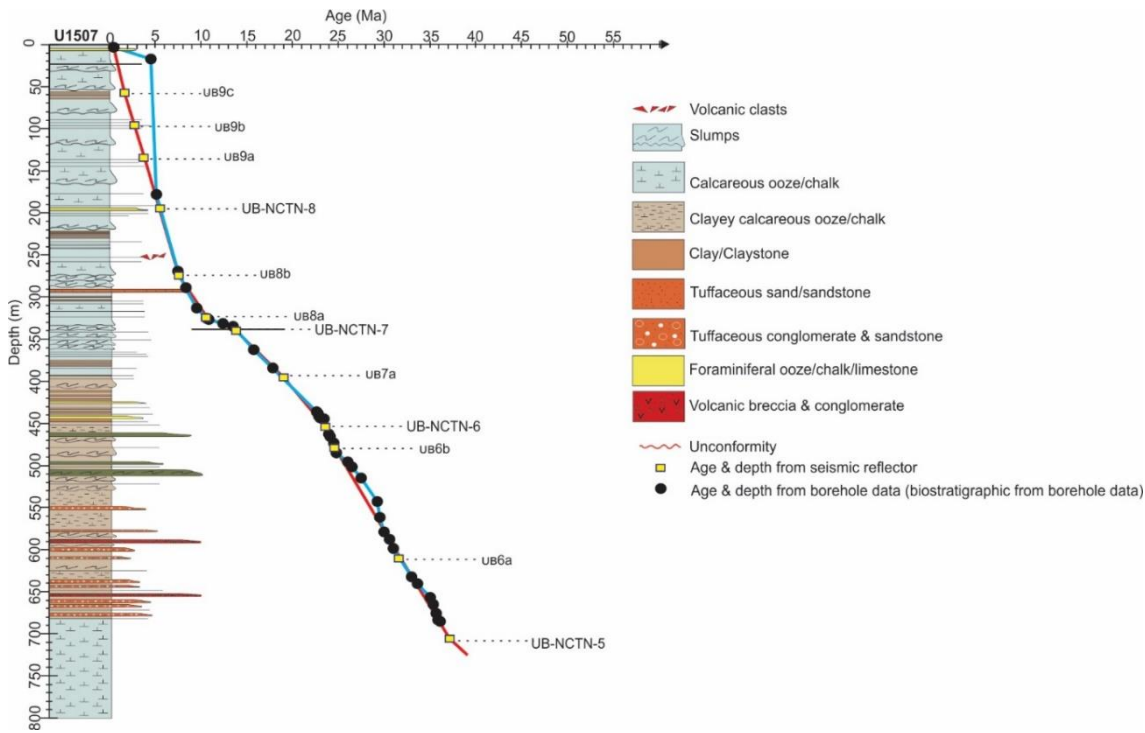


Figure S6. Borehole U1507.

Horizontal dash lines = seismic reflection/time horizons picked for units boundaries, red solid line=age model correlation for microfossil datum accounting for reworking (correction from U-NCTN-B9a to U-NCTN-B9c) and blue solid line= published age model from borehole data/sediment sampled at borehole U1507 (includes a single biostratigraphic datum that is inferred here to be reworked within a debris flow).

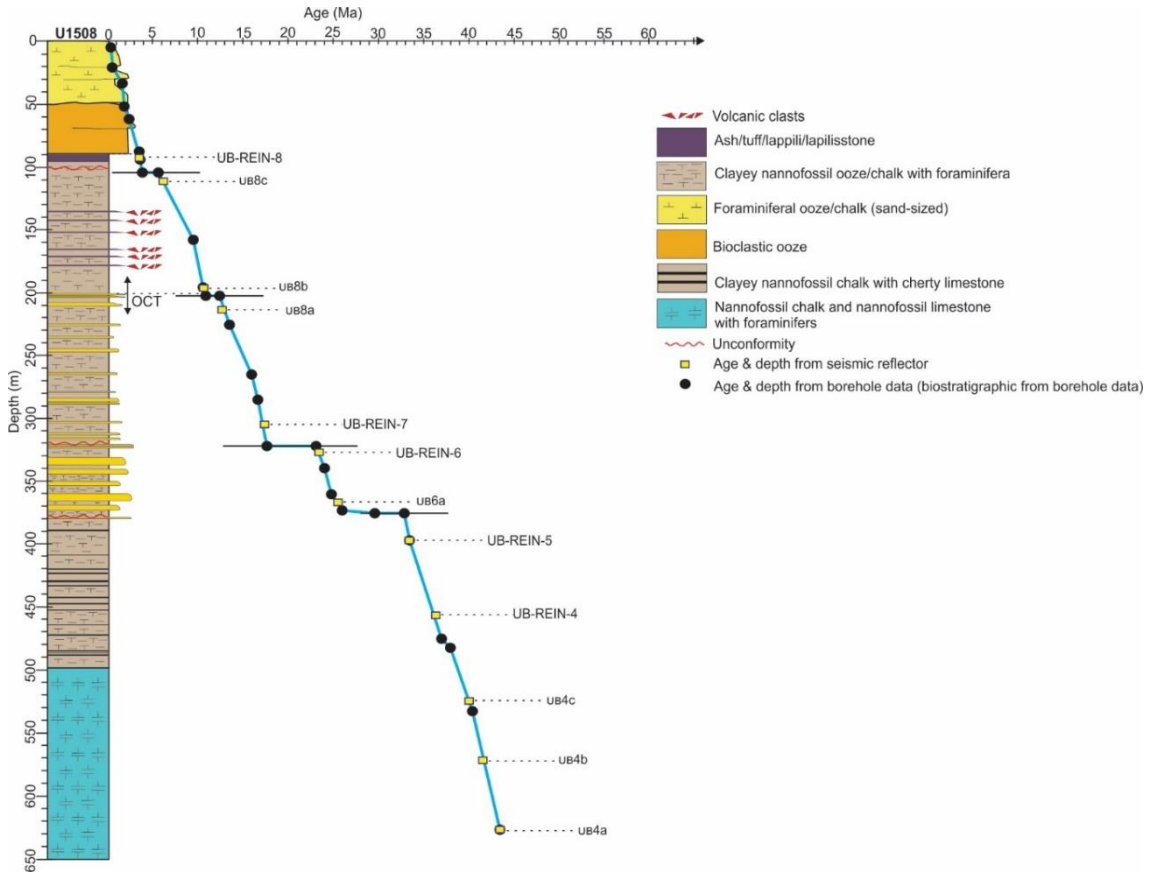


Figure S7. Borehole U1508.

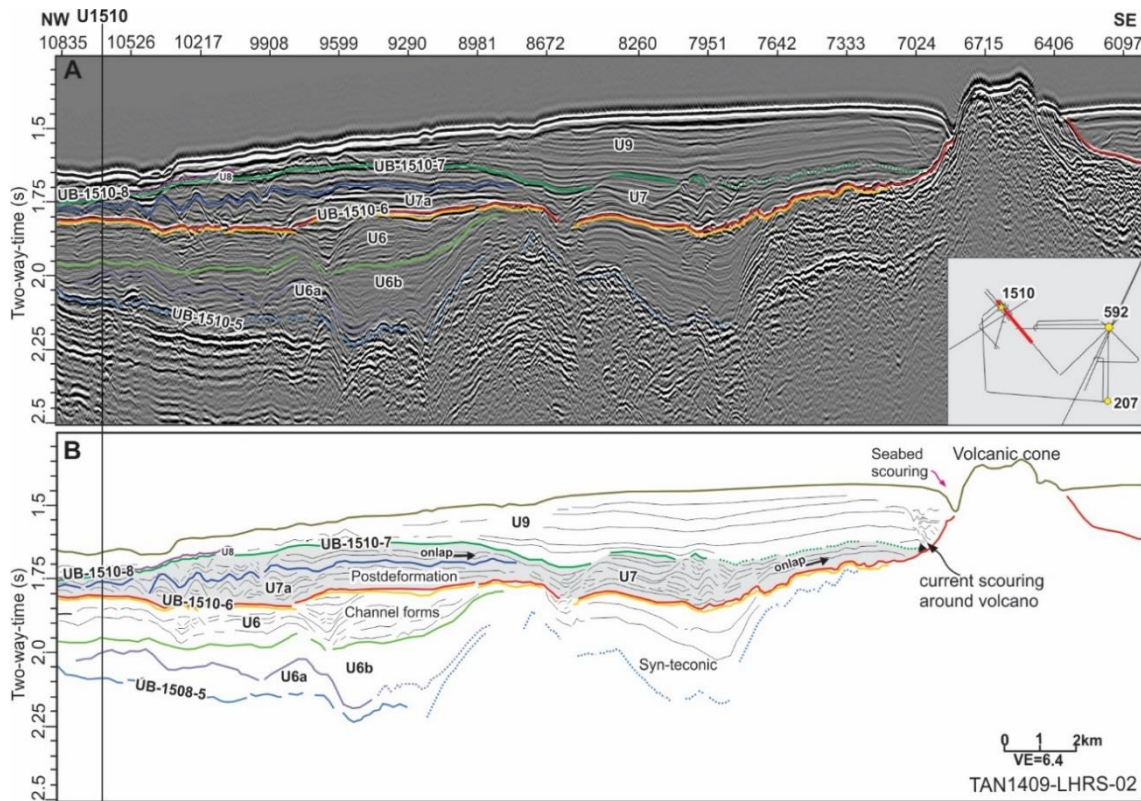


Figure S8. Southern Lord Howe Rise seismic reflection line TAN1409-LHRS-02 through borehole U1510, (A) seismic reflection image, and (B) illustrates Eocene reverse faulting, deformation, volcanism and erosional unconformity.

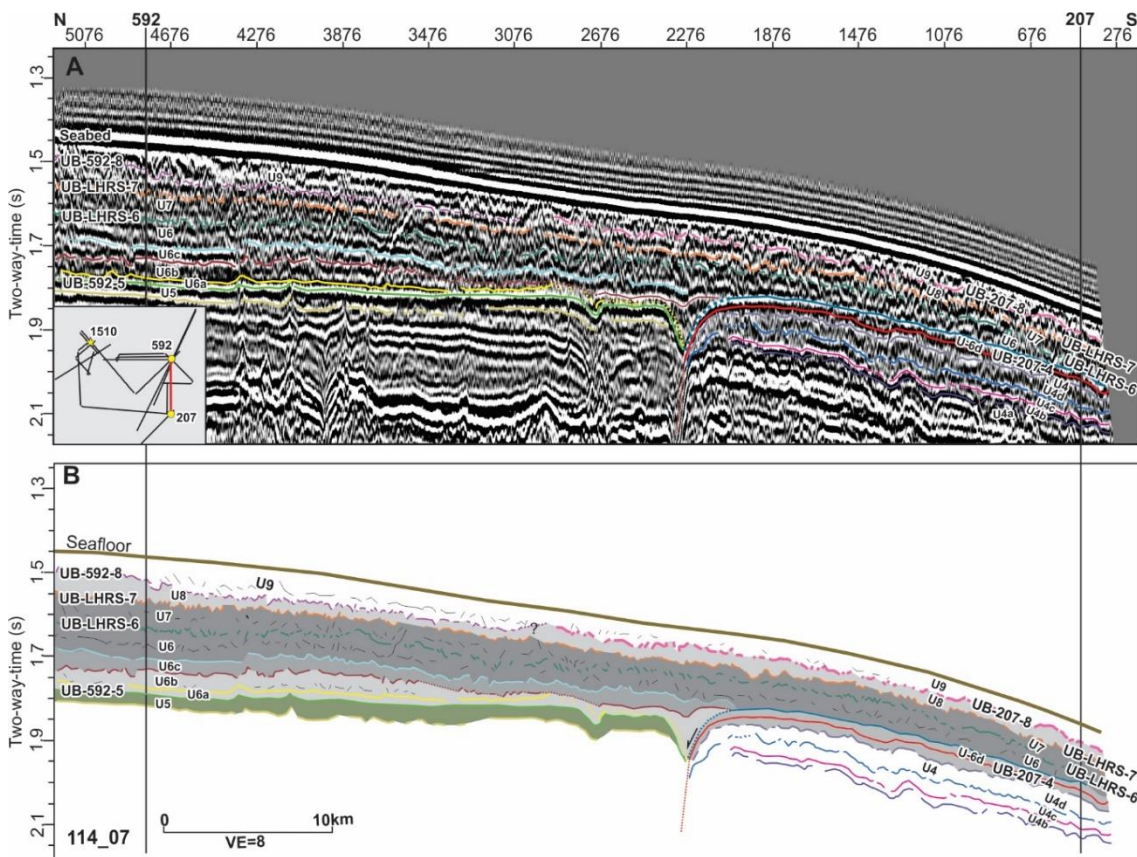


Figure S9. Southern Lord Howe Rise seismic reflection line 114_07 between Sites U592 and U207: (A) seismic reflection image, and (B) two sites show a lack of continuity of strata beneath a Miocene-Paleogene unconformity.

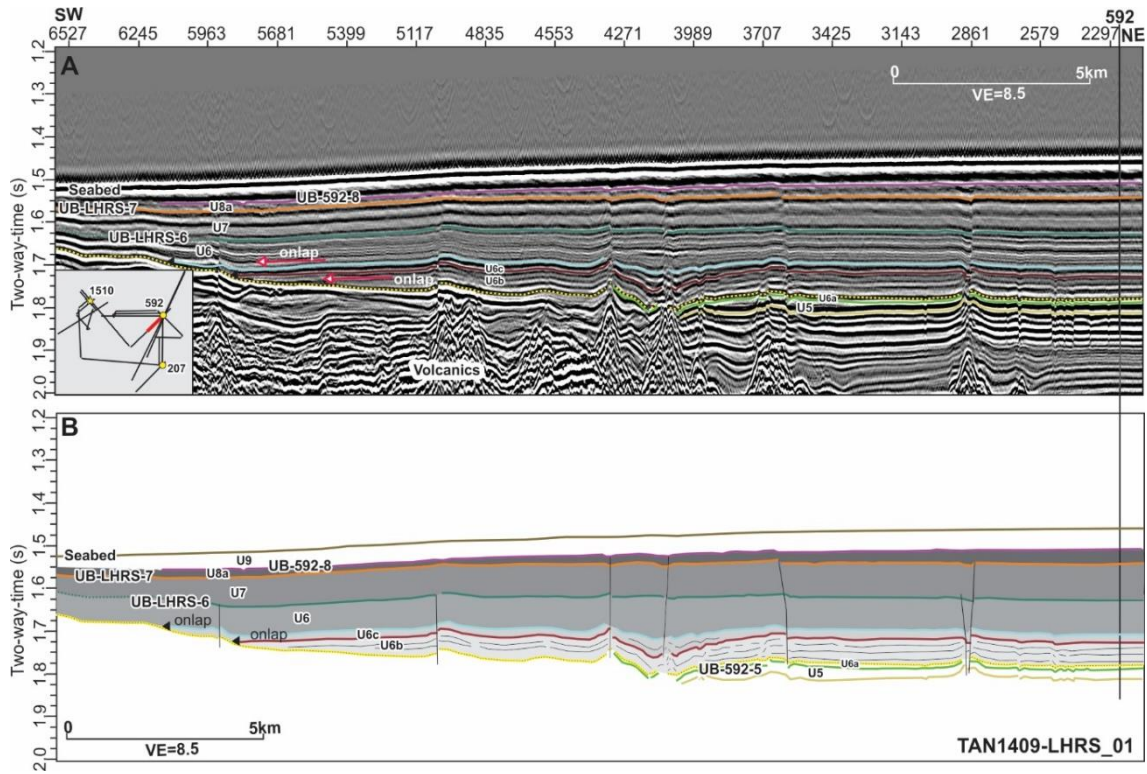


Figure S10. Southern Lord Howe Rise seismic line TAN1409-LHRS_01 near Site U592: (A) seismic reflection image, and (B) sketch of onlapping section just above Miocene unconformity (black yellow dash line).

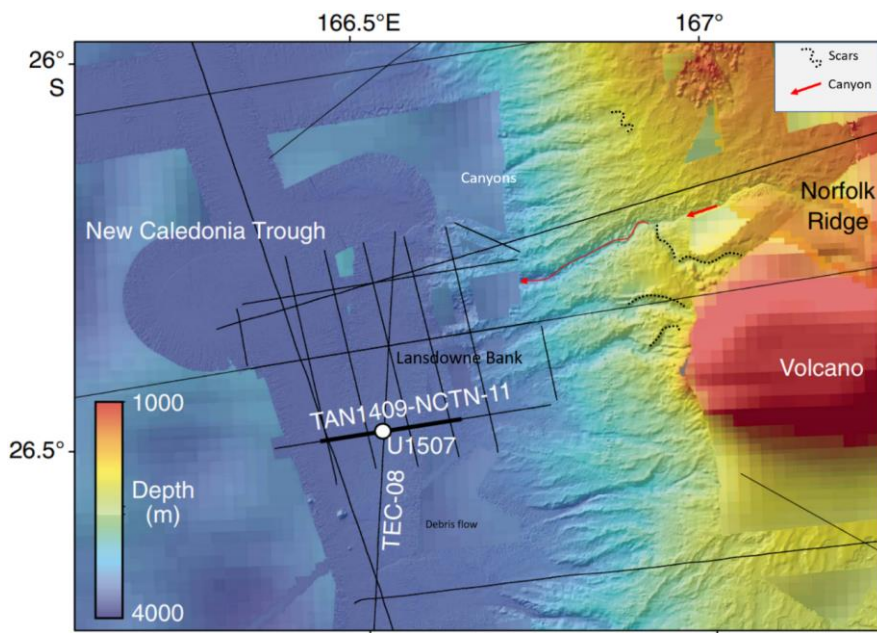


Figure S11. Bathymetric map showing local setting of Site U1507, with canyons and landslide scars on the adjacent flank of Norfolk Ridge.

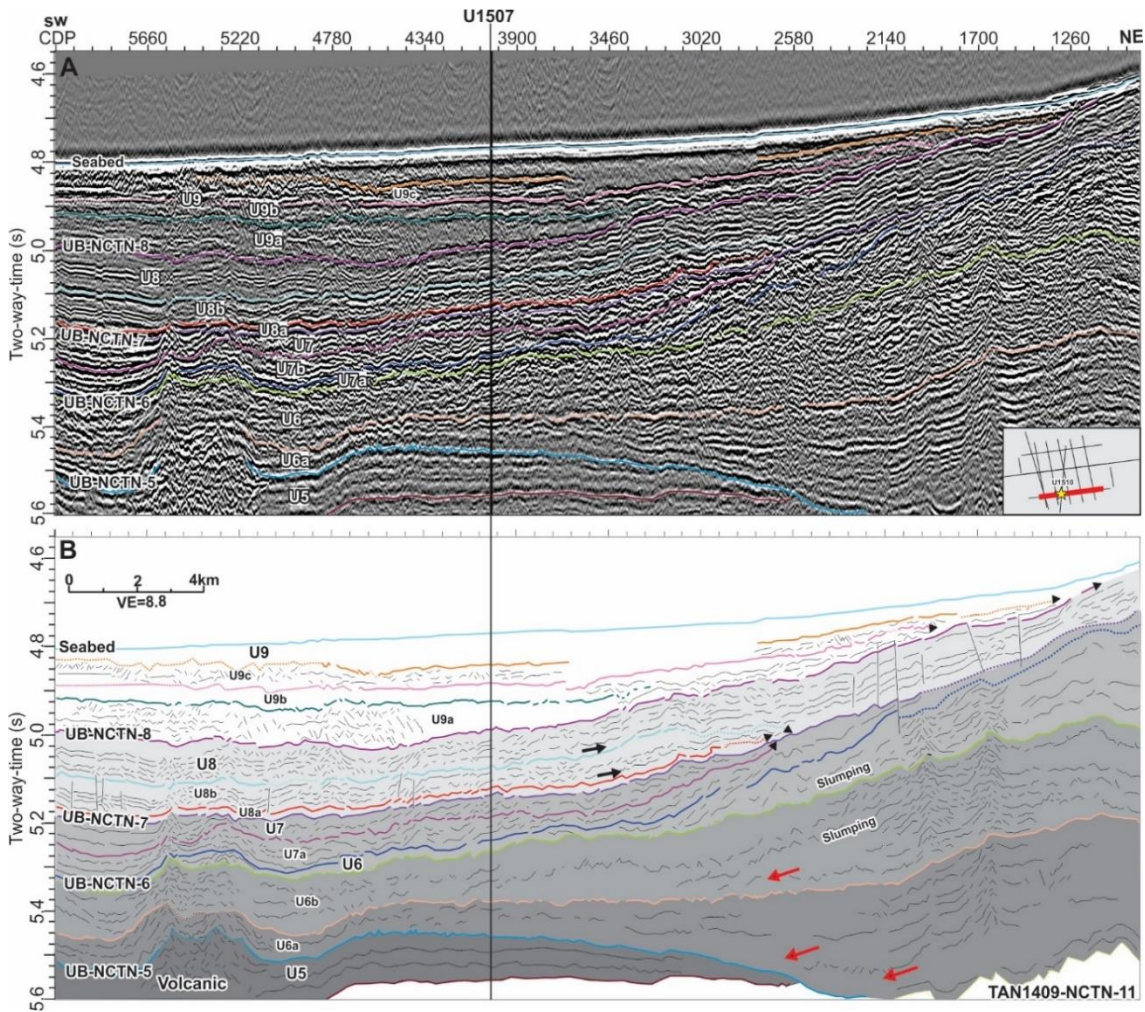


Figure S12. Seismic line line TAN1409-NCTN-11 at Site U1507, (A) seismic reflection image with horizons picked in colour, and (B) sketch of onlapping and downlapping strata near Site U1507. Stratigraphic onlaps are shown with small black arrow facing northeast and small two arrows with purple and blue colour are toplapping reflectors. Black line is polygonal faulting. Blank areas are transparent acoustically and interpreted as large-scale debris flows.

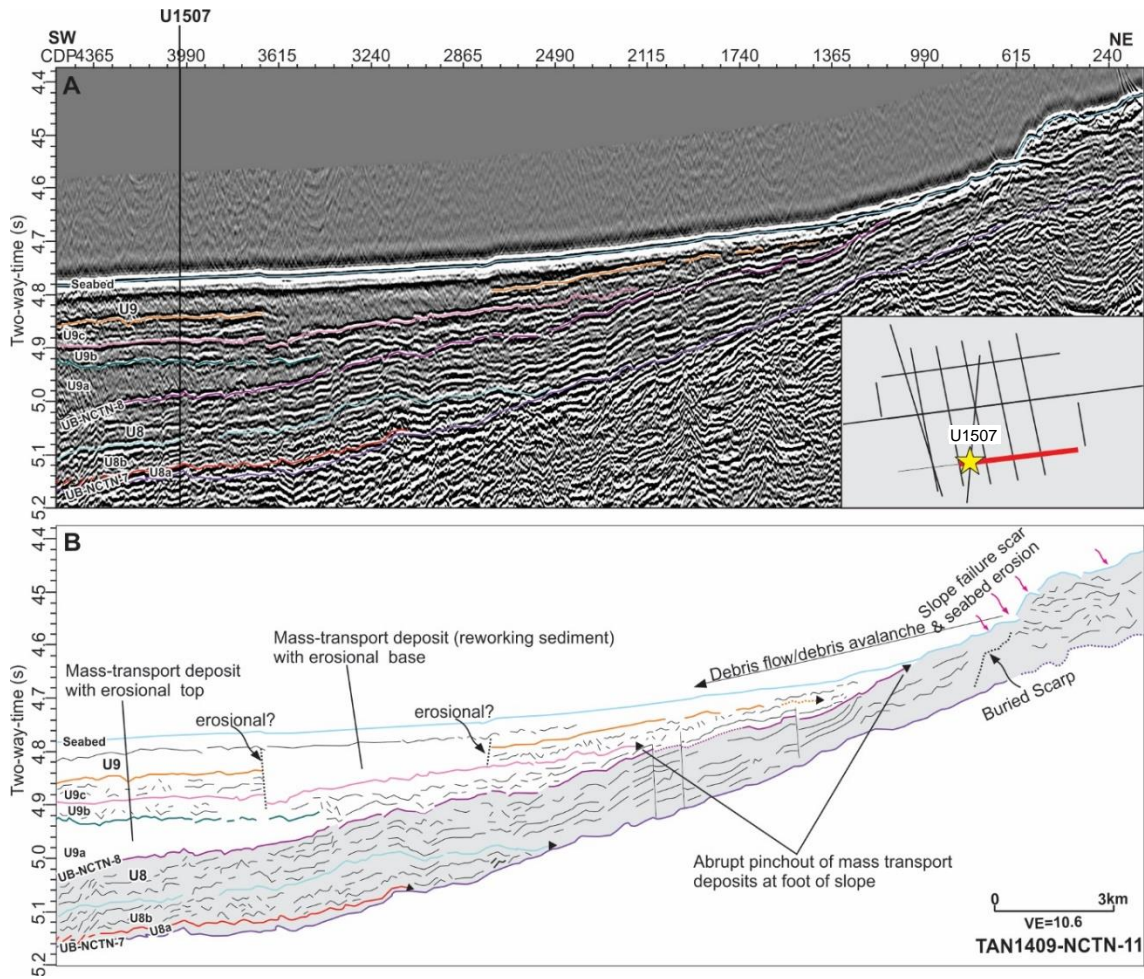


Figure S13. Seismic line TAN1409-011 near Site U1507 shows deposition of reworking sediment at the basin; (A) seismic reflection image, and (B) interpreted illustrating the relative position of slope failure scars at seabed and pinchout or onlap mass transport deposits at the edge of the basin, and buried escarpments on the slope.

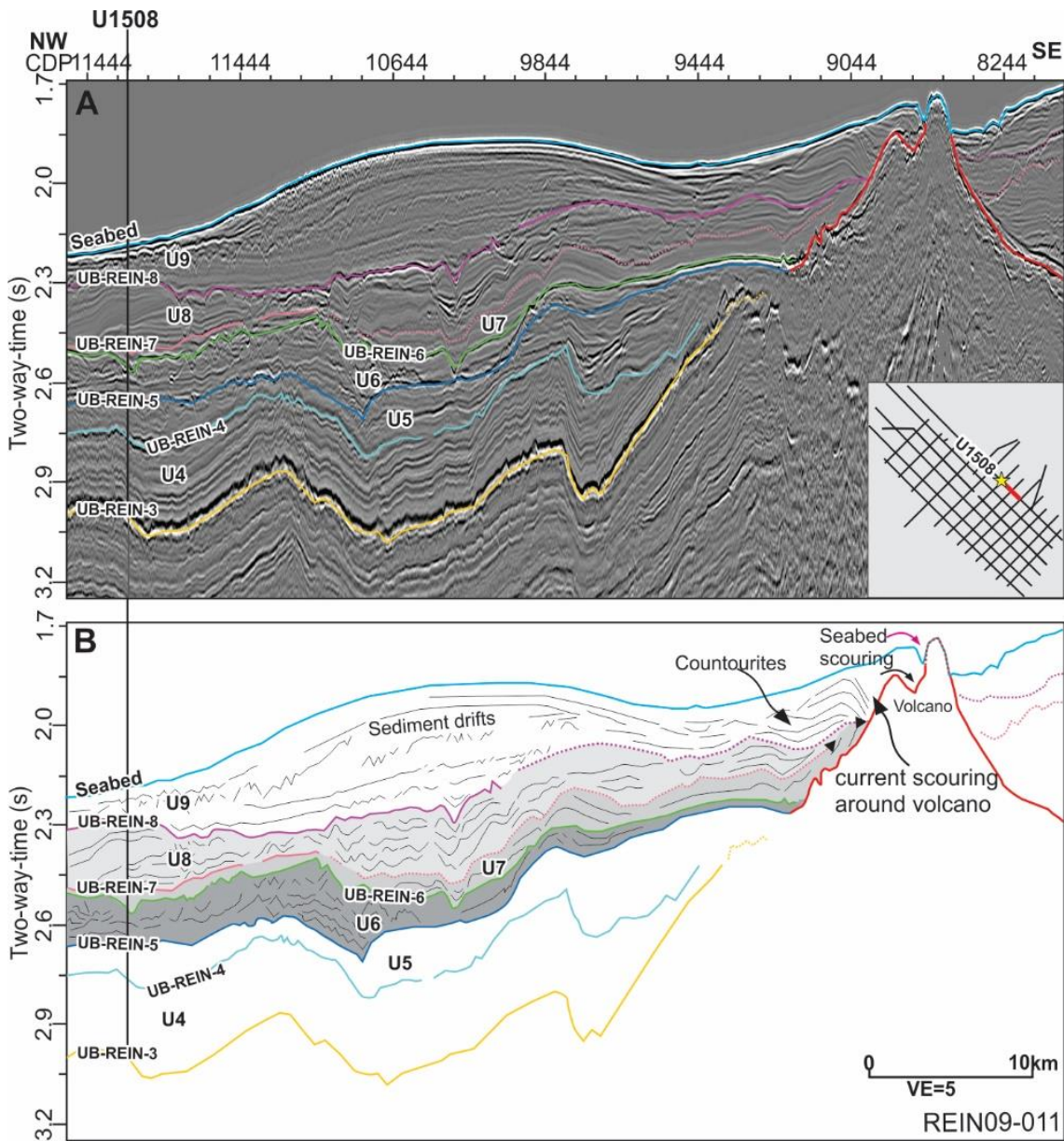


Figure S14. Reinga Basin seismic reflection line REIN09-011 illustrates horizons picked and seismic units near Site U1508: (A) seismic reflection image and, (B) interpreted seismic reflection presenting key seismic stratigraphic relationship along the strike. UB-REIN-5 appeared to correspond with the base strata, UB-REIN-6 and UB-REIN-7 onlap the volcano in the SE where seabed seems scouring against the volcano.

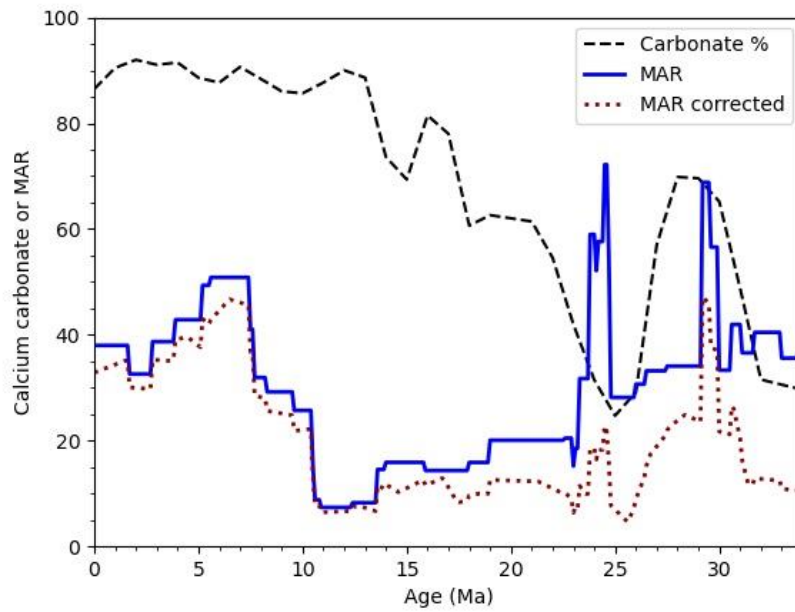


Figure S15. Site U1507 calcium carbonate (black dashed, wt %) values binned by sample age, averaged, and then interpolated to fill gaps. The NCTN average MAR curve (blue; Fig. 11) is corrected using the calcium carbonate curve to determine the carbonate component of MAR (red dotted; $\text{kg kyr}^{-1} \text{m}^{-2}$).

Table S1. Biostratigraphy for DSDP Leg 21 revised to be consistent with Sutherland et al. (2019).
 B = base, T = top, Bc = base common, Tc = top common.

Event	Zone	Age	U205		U206		U207		U208		U209		U210	
			m bsf	± m	m bsf	± m	m bsf	± m	m bsf	± m	m bsf	± m	m bsf	± m
B <i>Emiliana huxleyi</i>	NN21	0.29					6.00	6.00						
T <i>Dicoaster brouweri</i>	NN19	1.93			85.25	5.25	32.75	3.75	11.75	11.75	18.75	3.75	115.50	11.00
T <i>Discoaster pentraradiatus</i>	NN18	2.39			98.00	9.00	32.75	3.75	27.25	2.25	18.75	3.75	115.50	11.00
T <i>Discoaster surculus</i>	NN17	2.49			98.00	9.00	32.75	3.75	27.25	2.25	18.75	3.75	115.50	11.00
T <i>Discoaster tamalis</i>	NN17	2.80			115.25	9.75	41.00	6.00	35.25	7.25	27.75	3.75	170.00	9.50
T <i>Sphenolithus</i> spp.	NN17	3.54			148.49	6.98	47.00	1.50	55.25	5.25	40.50	4.50	170.00	9.50
T <i>Reticulofenestra pseudoumbilicus</i>	NN16	3.70			148.49	6.98	47.00	1.50	55.25	5.25	40.50	4.50	170.00	9.50
Bc <i>Discoaster asymmetricus</i>	NN14	4.13							64.25	5.25	40.50	4.50	217.00	39.00
T <i>Ceratolithus acutus</i>	NN14	5.04	29.63	10.13	168.49	14.52	73.25	18.75	95.25	5.25			341.71	10.28
B <i>Ceratolithus rugosus</i>	NN13	5.12	29.63	10.13	168.49	14.52	73.25	18.75	95.25	5.25			341.71	10.28
B <i>Ceratolithus acutus</i>	NN13	5.35	29.63	10.13	187.25	5.75	73.25	18.75	104.25	5.25			341.71	10.28
T <i>Discoaster quinqueramus</i>	NN12	5.59			187.25	5.75	73.25	18.75	118.50	10.50	48.92	3.92	341.71	10.28
B <i>Discoaster berggrenii</i>	NN11	8.29			195.75	5.25	95.75	5.25	191.75	9.75	124.42	73.08		
T <i>Discoaster hamatus</i>	NN10	9.53	68.75	2.25	207.00	4.50	113.99	5.02	227.25	5.25				
B <i>Discoaster hamatus</i>	NN9	10.55	77.75	8.25	215.25	5.25	118.25	0.75	248.75	11.75				
Tc <i>Discoaster kugleri</i>	NN8	11.58	101.00	4.50	225.75	6.75	118.25	0.75	248.75	11.75				
Bc <i>Discoaster kugleri</i>	NN7	11.90	119.00	15.00	247.25	8.75	121.44	3.94	275.25	16.25				
T <i>Sphenolithus heteromorphus</i>	NN6	13.53	166.75	14.25	292.75	3.75	121.42	3.92	306.49	16.49				
T <i>Heliocosphaera ampliapertura</i>	NN5	14.91	262.25	14.75	301.00	6.00	125.38	1.50	322.23	0.75				
Tc <i>Discoaster deflandrei</i>	NN5	15.80	262.25	14.75	301.00	6.00	125.38	1.50	322.23	0.75				
Bc <i>Sphenolithus heteromorphus</i>	NN5	17.71			301.00	6.00			336.49	15.01				
Tc <i>Sphenolithus belemnus</i>	NN4	17.95			301.00	6.00			336.49	15.01				
B <i>Sphenolithus belemnus</i>	NN3	19.03			301.00	6.00			364.48	14.48				
B <i>Discoaster druggii</i>	NN2	22.82	262.25	14.75	310.75	5.25			391.23	13.77				
Tc <i>Cyclicargolithus abisectus</i>	NN1	24.67	277.75	2.25	310.75	5.25			391.23	13.77				
T <i>Sphenolithus ciproensis</i>	NN1	24.43	282.25	3.75	405.50	6.00			419.69	16.19				
B <i>Sphenolithus ciproensis</i>	NP24	29.62	307.00	4.50	526.75	61.75			487.00	1.50				
B <i>Sphenolithus distentus</i>	NP24	30.00			612.98	2.02								
T <i>Reticulofenestra umbilicus</i>	NP23	32.02											491.00	46.50
T <i>Coccolithus formosa</i>	NP22	32.92											550.25	14.25
T <i>Chiasmolithus grandis</i>	NP18	37.98			612.98	2.02			487.00	1.50	228.25	32.25		
T <i>Chiasmolithus solitus</i>	NP17	40.40			635.23	21.73	138.94	12.06	487.75	0.75	284.00	1.50		
B <i>Reticulofenestra umbilicus</i>	NP16	42.77			673.48	18.03	169.75	2.25	489.25	2.25				
T <i>Chiasmolithus gigas</i>	NP15c	43.59					187.00	4.50	489.25	2.25				
B <i>Chiasmolithus gigas</i>	NP15b	45.59					194.50	4.50	529.49	11.49				
B <i>Blackites inflatus</i>	NP15a	47.84					224.25	8.75					572.00	9.00
B <i>Discoaster sublodoensis</i> (5-rayed)	NP14	48.48					235.25	4.75					615.50	10.50
B <i>Coccolithus crassus</i>	NP13	50.82			673.48	18.03	274.50	4.50						
B <i>Discoaster lodoensis</i>	NP12	53.70			698.75	8.75	290.25	3.75						
B <i>Discoaster diastypus</i>	NP11	54.95							529.49	11.49				
B <i>Rhomboaster</i> spp.	NP10	55.96							529.49	11.49				
B <i>Discoaster multiradiatus</i>	NP9	57.21							543.23	3.75				
B <i>Discoaster mohleri</i>	NP9	58.97					297.00	4.50						
B <i>Heliolithus kleinPELLI</i>	NP6	59.54					297.00	4.50						
B <i>Fasciculithus tympaniformis</i>	NP5	61.51			698.75	8.75	297.00	4.50	543.23	3.75				
B <i>Cruciplacolithus tenuis</i>	NP3	65.47					297.00	4.50	569.25	8.25				
B <i>Nephrolithus frequens</i>	NC23	67.84							585.00	4.50				

Table S2. Biostratigraphy for DSDP Leg 90 revised to be consistent with Sutherland et al. (2019).

B = base, T = top.

Event	Zone	Age	U587		U588		U589		U590		U591		U592		U593	
			m bsf	± m	m bsf	± m	m bsf	± m	m bsf	± m	m bsf	± m	m bsf	± m	m bsf	± m
B <i>Emiliana huxleyi</i>	NN21	0.29	7.95	7.95	1.61	0.75	2.26	0.75	3.80	0.75	3.23	0.18	3.77	0.73	4.07	1.03
T <i>Emiliana ovata</i>	NN20		16.90	1.00	3.11	0.75			6.53	0.47	7.94	1.50	4.52	0.02	9.64	1.50
T <i>Discoaster brouweri</i>	NN19	1.93	29.10	0.75	20.45	0.75	16.91	0.00	35.83	0.03	49.62	1.78	21.03	0.89	43.70	0.20
T <i>Discoaster pentaradiatus</i>	NN18	2.39	30.88	1.03	25.56	0.75			46.21	0.75	62.54	1.50	24.49	0.75	44.47	0.57
T <i>Discoaster surculus</i>	NN17	2.49	32.44	0.53	27.06	0.75			46.21	0.75	65.54	1.50	25.99	0.75	45.79	0.75
T <i>Amaurolithus tricorniculatus</i>	NN16	3.70	46.80	0.75	75.06	0.75			131.51	0.30	146.22	0.02	69.92	1.78	86.72	4.82
T <i>Reticulofenestra pseudoumbilicus</i>	NN15	3.92	38.70	0.75	50.76	0.75			87.56	0.75	103.44	1.00	31.99	0.75	68.17	2.37
B <i>Discoaster asymmetricus</i>	NN14	4.13	51.90	0.75	92.76	0.75			151.76	0.75	186.32	2.52	119.72	0.02	120.32	0.02
B <i>Ceratolithus rugosus</i>	NN13	5.12	54.90	0.75	92.76	0.75			172.51	0.75	191.57	1.73				
T <i>Discoaster quinqueringus</i>	NN12	5.59	56.40	0.75	102.35	0.75			196.21	0.75	213.64	1.50	129.32	0.02	203.42	3.28
B <i>Discoaster quinqueringus</i>	NN11a	8.11	91.21	1.50	187.71	0.30			324.53	1.77	308.83	0.02	169.24	1.50	227.44	1.50
T <i>Discoaster hamatus</i>	NN10	9.53			212.46	0.75			353.33	1.77	347.58	0.77	186.92	0.02	243.32	1.78
B <i>Discoaster hamatus</i>	NN9	10.55			230.16	0.75			377.33	3.03	370.83	4.77	206.12	0.02	254.72	0.02
B <i>Catinaster coalitus</i>	NN8	10.89			234.96	1.05			383.93	0.03	375.62	0.02	207.64	1.50		
B <i>Discoaster kugleri</i>	NN7	11.90			250.36	0.26			414.26	1.50	385.22	0.02	225.32	0.02	342.64	1.50
T <i>Sphenolithus heteromorphus</i>	NN6	13.53			280.58	0.02			436.46	1.50	437.74	1.50	255.64	1.50	394.25	0.36
B <i>Discoaster exilis</i>					315.31	0.00			460.73	0.03	490.82	0.02	268.24	1.50	408.32	0.02
T <i>Sphenolithus belemnus</i>	NN4	17.95			322.06	0.75			470.33	0.03			287.44	1.50	416.12	1.78
T <i>Triquetrorhabdulus carinatus</i>	NN3	18.28			333.46	1.04			487.73	1.77			296.04	0.50	435.32	1.78
B <i>Discoaster druggii</i>	NN2	22.82			344.97	0.64			491.06	1.50			305.89	0.75	437.12	0.02
T <i>Helicosphaera recta</i>	NN1	23.20			354.46	0.75									470.44	1.50
T <i>Sphenolithus delphix</i>	NN2	23.11			363.96	0.85										
B <i>Sphenolithus delphix</i>	NN2	23.21			398.81	0.71										
T <i>Sphenolithus ciperoensis</i>	NN1	24.43			404.67	1.46										
T <i>Sphenolithus distentus</i>	NP25	26.84			460.81	1.50										
T <i>Sphenolithus predistentus</i>	NP25	26.93			460.81	1.50									507.87	3.52
B <i>Sphenolithus ciperoensis</i>	NP24	29.62			463.61	1.29										
T <i>Reticulofenestra umbilicus</i>	NP23	32.02													525.04	1.50
T <i>Isthmolithus recurvus</i>	NP23	32.49											306.23	0.43	525.04	1.50
T <i>Coccolithus formosus</i>	NP22	32.92											321.10	0.24	534.64	1.50
T <i>Discoaster saipanensis</i>	NP21	34.44											341.45	0.89	561.02	0.95
T <i>Discoaster barbadiensis</i>	NP21	34.76											341.45	0.89	566.46	1.51

Table S3. Ages assigned to reflectors, northern Lord Howe Rise.

Name	Age
seabed	0.0
UB-LHRN-9a-5	2.4
UB-1506-9b	2.8
UB-LHRN-9a-4	3.6
UB-LHRN-9a-3	4.5
UB-LHRN-9a-2	5.2
UB-LHRN-9a-1	5.6
UB-LHRN-8	6.7
UB-LHRN-8b	8.0
UB-LHRN-8a	9.0
UB-LHRN-7	11.9
UB-LHRN-7b	13.5
UB-LHRN-7a	18.0
UB-LHRN-6	22.5
UB-LHRN-6a	25.5
UB-LHRN-5	44.0

Table S4. Ages assigned to reflectors, southern Lord Howe Rise.

Name	Age
seabed	0.00
207-U10	2.44
U1510-U07	3.61
LHRS_U08	4.80
LHRS_U07	7.00
U1510-U06	8.23
U1510-U5C	13.97
U1510-U5B	17.81
U1510-U3B	36.28
U1510-U2B	42.71
U1510-U2A	46.02
207-U5E	9.34
207-U5D	12.74
207-U2E	40.63
207-U2D	41.60
207-U2B	47.03
207-U2A	48.34
592-U6C	11.65
592-U6B	12.90
592-U6A	18.04
592-U04	32.53
592-U3B	34.26

Table S5. Ages assigned to reflectors, northern New Caledonia Trough.

Name	Age
seabed	0
U1507_R9N	1.67
U1507_R9M	2.78
U1507_R9L	3.84
U1507_R9K	5.51
U1507_R9J	7.62
U1507_R9I	10.48
U1507_R9H	13.94
U1507_R9G	18.95
U1507_R9F	23.72
U1507_R9E	24.64
U1507_R9D	31.69
U1507_R9C	37.13
U1507_R9B	43.72
U1507_R9A	57.07

Table S6. Ages assigned to reflectors, Reinga Basin.

Name	Age
seabed	0.00
RB_02A	3.66
RB_04	6.12
RB_06	10.61
RB_08	12.82
RB_09	17.26
RB_10	23.42
RB_11	25.50
RB_13	33.43
RB_14	36.17
RB_15	40.01
RB_16	41.60
RB_17	43.42
RB_18	53.13

REFERENCES

Sutherland, R., Dickens, G. R., Blum, P., Agnini, C., Alegret, L., Asatryan, G., Bhattacharya, J., Bordenave, A., Chang, L., Collot, J., Cramwinckel, M. J., Dallonave, E., Drake, M. K., Etienne, S. J. G., Giorgioni, M., Gurnis, M., Harper, D. T., Huang, H.-H. M., Keller, A. L., Lam, A. R., Li, H., Matsui, H., Morgans, H. E. G., Newsam, C., Park, Y.-H., Pascher, K. M., Pekar, S. F., Penman, D. E., Saito, S., Stratford, W. R., Westerhold, T., and Zhou, X., 2019, International Ocean Discovery Program Expedition 371: Tasman Frontier Subduction Initiation and Paleogene Climate, College Station, TX, USA, International Ocean Discovery Program, Proceedings of the International Ocean Discovery Program, 318 p.: